Dynamic Covalent Chemistry Hot Paper

How to cite: *Angew. Chem. Int. Ed.* **2023,** *62,* e202214495
International Edition: doi.org/10.1002/anie.202214495
German Edition: doi.org/10.1002/ange.202214495

Light-Fueled Transformations of a Dynamic Cage-Based Molecular System

Marco Ovalle, Michael Kathan, Ryojun Toyoda, Charlotte N. Stindt, Stefano Crespi, and Ben L. Feringa**

Abstract: In a chemical equilibrium, the formation of high-energy species—in a closed system—is inefficient due to microscopic reversibility. Here, we demonstrate how this restriction can be circumvented by coupling a dynamic equilibrium to a light-induced *E*/*Z* isomerization of an azobenzene imine cage. The stable *E*-cage resists intermolecular imine exchange reactions that would "open" it. Upon switching, the strained *Z*-cage isomers undergo imine exchange spontaneously, thus opening the cage. Subsequent isomerization of the *Z*-open compounds yields a high-energy, kinetically trapped *E*-open species, which cannot be efficiently obtained from the initial *E*-cage, thus shifting an imine equilibrium energetically uphill in a closed system. Upon heating, the nucleophile is displaced back into solution and an opening/closing cycle is completed by regenerating the stable all-*E*-cage. Using this principle, a light-induced cage-to-cage transformation is performed by the addition of a ditopic aldehyde.

Introduction

The study of fundamental processes that sustain life is an exciting and inspiring topic across every scientific discipline. For chemists, the intricacy and beauty of molecular machinery inside all forms of life[1,2] has served as an inexhaustible source of inspiration for fascinating designs, such as artificial molecular machines (AMMs).[3–13] Aided by molecular motors,[14–18] pumps,[19–22] and switches,[18,23] chemists have been able to create elegant systems that, although still far from the complexity of their biological counterparts, might be able to satisfy the needs of our society in the near future and thus start to pave the way for artificial machinery and responsive materials.

In this regard, an important aspect to understand is the transformation and use of energy by molecular machines. In nature, the fuel that powers most biological processes, adenosine triphosphate (ATP), is constantly being consumed and generated by recycling its waste products, adenosine diphosphate (ADP) and inorganic phosphorus (P_i).

Thermodynamically disfavored transformations, such as the conversion from waste back into fuel, is a challenging process in a closed system. The principle behind this limitation is microscopic reversibility[24] which states that the transition state (and therefore pathway) for every elementary step in a chemical reaction is the same in the forward and backward direction. As a result, high-energy states cannot be preferably populated by thermodynamic means, rendering endergonic reactions highly inefficient or unattainable.[25,26] Sheer input of energy is often not enough to overcome this limitation; it is the coupling of this endergonic to a secondary exergonic process that can drive a disfavored reaction. Following the previous example of ATP, during photosynthesis, light is used as an energy source to create an electrochemical proton gradient across the thylakoid membrane of the chloroplasts.[27] This gradient fuels the biological molecular machine ATP synthase, which drives the endergonic conversion of ADP into ATP.[28]

The use of light as a power source and an external stimulus for dynamic transformations has certain key advantages, such as applicability with high spatiotemporal precision and the lack of chemical waste products.[29] Molecular photoswitches are attractive synthetic tools that use light as an energy source to induce a reversible change

[*] M. Ovalle, Dr. M. Kathan, Dr. R. Toyoda, C. N. Stindt, Dr. S. Crespi, Prof. Dr. B. L. Feringa
Stratingh Institute for Chemistry, University of Groningen
Nijenborgh 4, 9747AG Groningen (The Netherlands)
E-mail: b.l.feringa@rug.nl

Dr. M. Kathan
Present address: Department of Chemistry, Humboldt-Universität zu Berlin
Brook-Taylor-Str. 2, 12489 Berlin (Germany)
E-mail: michael.peter.kathan@chemie.hu-berlin.de

Dr. R. Toyoda
Present address: Department of Chemistry, Graduate School of Science, Tohoku University
6-3 Aramaki-Aza-Aoba, Aobaku, Sendai 980-8578 (Japan)

Dr. S. Crespi
Present address: Department of Chemistry-Ångström Laboratory, Uppsala University
Box 523, 75120 Uppsala (Sweden)

in their properties. The development of molecular machines by the incorporation of photoswitches in more complex molecular systems and architectures, such as macrocycles and molecular cages, has the potential to exhibit emergent behaviors that resemble their biological counterparts.[30–45]

An example of this emergent behavior is the influence of switching in the reactivity of constrained molecular architectures. Particularly, the effect of the geometric change in the switch can introduce strain in the macrocycle, and by doing so, it can promote the reactions in which the strain directly affects the rate limiting step.[46–48]

Dynamic covalent chemistry, specifically reversible imine bond formation, offers not only useful scaffolds for the manipulation of constrained chemical systems but it is also an efficient method to generate molecular cages and macrocycles.[49–51] The reversible imine bond formation serves as an "error checking" mechanism that favors the thermodynamically most stable assembly, which—with the right molecular building blocks—yields a cage or macrocyclic compound. Consequently, the final assembly is sensitive to changes in the environment that affect the thermodynamic stability of the product. An example of the dynamic behavior of imine cages is the cage-to-cage transformation process,[52] in which a self-assembled cage can be converted into a different cage architecture in the presence of a competing building block or by a change in its properties in response to an external stimulus. By the same principle, other post-synthetic cage and macrocycle transformations are possible, such as cage catenation, cage-to-framework, cage-to-composite, macrocycle-to-polymer, macrocycle-to-macrocycle, etc.[53–62] This dynamic behavior of imine self-assemblies makes them attractive discrete molecular architectures to build photoresponsive molecular machines. We anticipated that the introduction and operation of molecular switches in an imine cage architecture could be coupled to energetically demanding and reversible light-induced transformations.

Herein, we report a new type of light-driven molecular machine based on a macrobicyclic imine cage (**1**, Figure 1) comprising three constrained photoswitchable azobenzene units. The use of light as an energy source allows an endergonic transformation to occur in an imine/amine exchange, which results in the operation of a 4-step cycle in which the cage is "opened" and "closed" sequentially.

The design and operational mechanism of the system are shown in Figure 1. In step I, starting with the all-*E* cage **1-*EEE***, the azobenzene switches undergo a photochemical *E*/*Z* isomerization without changing the bond connectivity, following a stepwise transition from **1-*EEE*→1-*ZEE*→1-*ZZE*→1-*ZZZ*** upon UV light irradiation (λ_{irr} = 340 nm; Figure 1, step I). In the reverse reaction, the *Z*→*E* isomerizations of the azobenzenes in cage **1** occur spontaneously, being accelerated by visible light irradiation (λ_{irr} = 420 nm) or heating in a stepwise manner from **1-*ZZZ*→1-*ZZE*→1-*ZEE*→1-*EEE*** (step I′). Although the isomerization process occurs without breaking the imine bonds, it has a direct impact on the thermodynamic stability of the imine bonds in the cage. While **1-*EEE*** is highly stable, the *Z* isomers of **1** are less stable due to the geometrical change in the constrained bicyclic structure that builds-up tension in the imine bonds. This strained structure is prone to relax to a less energetic resting state, which can either occur by *Z*/*E* isomerization to regain **1-*EEE*** (step I′) or by breaking the macrobicyclic structure in a nucleophile/imine exchange with a competing nucleophile to form an "open cage" **Open 1** (step II). Since we perform this reaction from the photostationary state of **1** after UV light irradiation (**1-PSS$_{340}$**, λ_{irr} = 340 nm), we refer to this mixture of isomers as **Open 1-PSS$_{340}$**. This mixture is enriched with *Z* azobenzene isomers, therefore, we can rapidly photoisomerize the switches using visible light (λ_{irr} = 420 nm). This is a pathway to populate and observe the thermodynamically disfavored, high-energy state **Open 1-*EEE*** in a higher abundance than the one accessible by sheer input of thermal energy. The same *Z*/*E* isomerization of the azobenzene can occur thermally, thus, leading to the same high energy species.

Finally, relaxation of **Open 1-*EEE*** yields initial and thermodynamically most stable **1-*EEE*** spontaneously (step IV) by the now favored (and exergonic) intramolecular nucleophile/imine exchange from **Open 1-*EEE*→1-*EEE*** that releases the nucleophile back into the mixture. In this 4-step transformation (or cage opening/closing) cycle, a nucleophile/imine reaction is actively driven away from its equilibrium composition by light.

This principle was used to facilitate a light-induced cage-to-cage transformation in the presence of a competing ditopic aldehyde and water to form cage **2** (Figure 1, step V). Similar to the cage opening/closing cycle, cage **1-*EEE*** is stable and the cage-to-cage transformation is negligible even after prolonged heating in the dark. However, after irradiation, the system undergoes a cage-to-cage transformation.

Results and Discussion

Cage **1** was synthesized by the condensation of (*E*)-3,3′-(diazene-1,2-diyl)dibenzaldehyde (**3-*E***) with tris(2-aminoethyl)amine (**TREN**) and characterized by NMR and UV/Vis spectroscopy as well as X-ray crystal structure analysis (Supporting Figures S1–S6). To elucidate the operational mechanism of our system, each step of the cage opening/closing cycle was studied by time-resolved NMR and UV/Vis spectroscopy. To compare the constrained cage to an unconstrained linear system, 3,3′-bis(*n*-butylimine)azobenzene **4** was synthetized as a reference compound (Supporting Figures S7–S9).

Step I. 1-EEE→1-PSS$_{340}$ photoisomerization

In order to study the photoswitching of **1-*EEE***, which corresponds to step I and I′ (Figures 1 and 2) in the cage opening/closing cycle, the isomerization process was studied by UV/Vis (Supporting Figure S10) and ^{1}H NMR spectroscopy (step I, Figures 2a and b, Supporting Figures S11–S18). The evolution of the ^{1}H NMR spectrum under constant irradiation (λ_{irr} = 340 nm, 11.3 h) allowed us to assign the signals to the corresponding isomer of **1** by

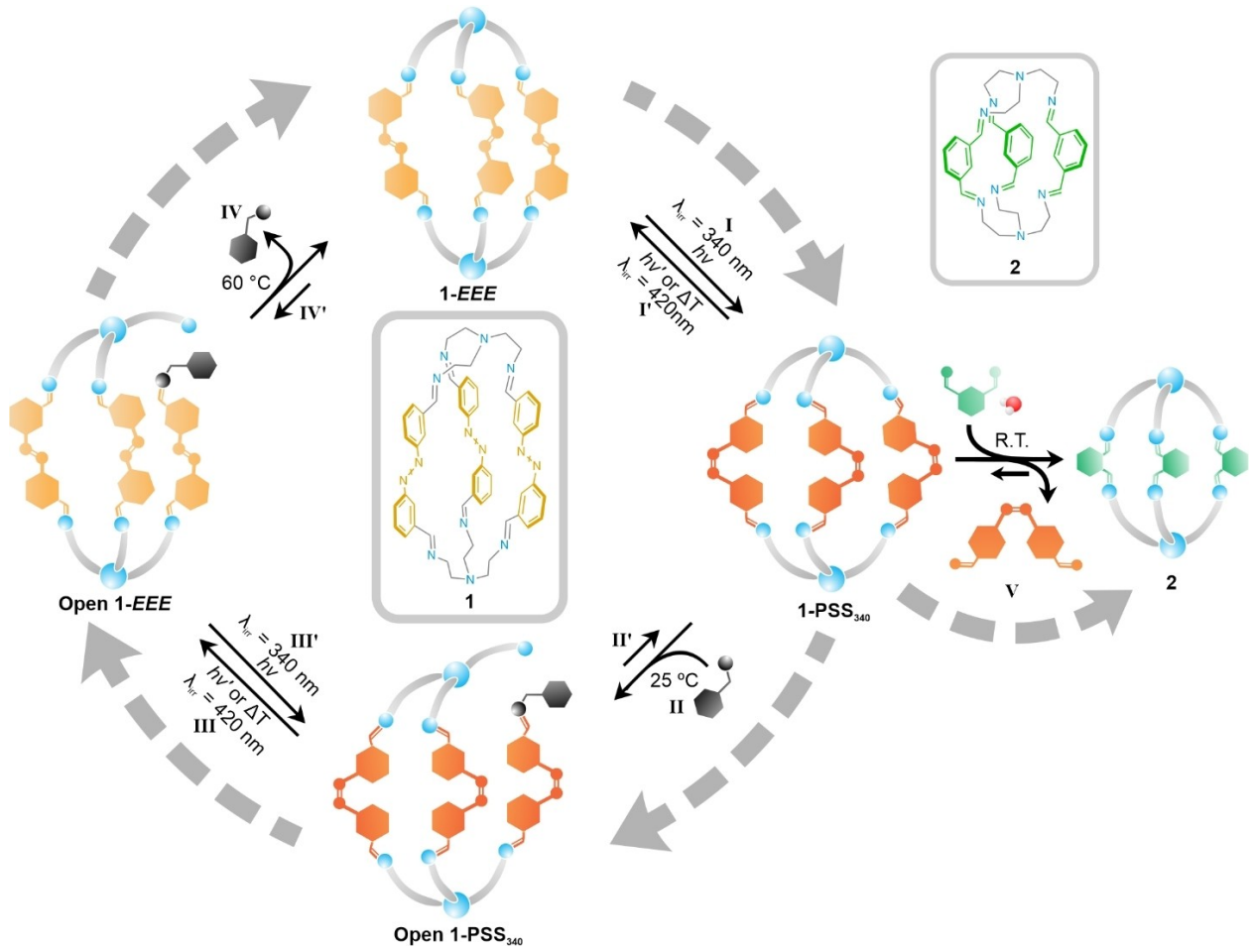

Figure 1. Light-induced transformation of **1**. The self-assembled cage **1-*EEE*** is highly stable and the intermolecular nucleophile/imine exchange rate is low. Upon irradiation (step I), the cage is converted into its less stable *Z* isomers **1-PSS$_{340}$** (**1-*ZZZ***, **1-*ZZE*** and **1-*ZEE***) that can now react with a competing nucleophile, such as an amine (black, step II). The product of this transformation is referred to as **Open 1-PSS$_{340}$**. Relaxation of the switches by either visible-light irradiation or thermal relaxation forms **Open 1-*EEE*** (step III), a kinetically trapped, high-energy state. Spontaneous intramolecular amine/imine exchange releases the competing nucleophile and regenerates thermodynamically stable cage **1-*EEE*** (step IV). When a ditopic aldehyde (green) is introduced into the system, aided by a nucleophile such as water, a light-induced cage-to-cage transformation is observed (step V).

analyzing their kinetic profiles of isomerization (Figure 2c, Supporting Figures S11–S18). With this information, we were able to determine the distribution of isomers of the mixture **1-PSS$_{340}$** in benzene-d_6. It consists of fully switched isomer **1-*ZZZ*** (68 %, Figure 2, green), the partially switched isomers **1-*ZZE*** (18 %, Figure 2, brown), **1-*ZEE*** (9 % Figure 2, red) and non-switched cage **1-*EEE*** (5 %, Figure 2, blue). The obtained kinetic profile revealed that the *E*→*Z* photoisomerization step proceeds in a stepwise and sequence specific manner following the transformations **1-*EEE*→1-*ZEE*→1-*ZZE*→1-*ZZZ*** (Figure 2c, Supporting Figures S11–S18).

Step I′. 1-PSS$_{340}$→1-EEE isomerization

For the Z/*E* isomerization of **1**, the transformation from mixture **1-PSS$_{340}$** to **1-*EEE*** (step I′, Figure 2d) was studied. This process can proceed either thermally (Supporting Figures S19–S22) or photochemically with visible light irradiation (λ_{irr} = 420 nm, Figure 2d, Supporting Figure S23 and S24). For the thermal relaxation pathway, the kinetic analysis (Supporting Figure S25) shows a similar sequence-specific trend and only **1-*EEE*** is observed at thermal equilibrium. Interestingly, the mono switched isomer **1-*ZEE*** has a thermal relaxation rate that is approximately one order of magnitude larger than the ones of **1-*ZZE*** and **1-*ZZZ***. The PSS at 420 nm is referred to as **1-PSS$_{420}$** and it contains mostly **1-*EEE*** and approximately 15 % of the mono switched isomer **1-*ZEE***.

Step II. 1-PSS$_{340}$→Open 1-PSS$_{340}$ exergonic intermolecular amine/imine exchange

After analyzing the isomerization of **1**, the reactivity of the irradiated sample with amines was studied. The mixture **1-PSS$_{340}$** (0.8 mmol in C_6D_6) was reacted with 2-meth-

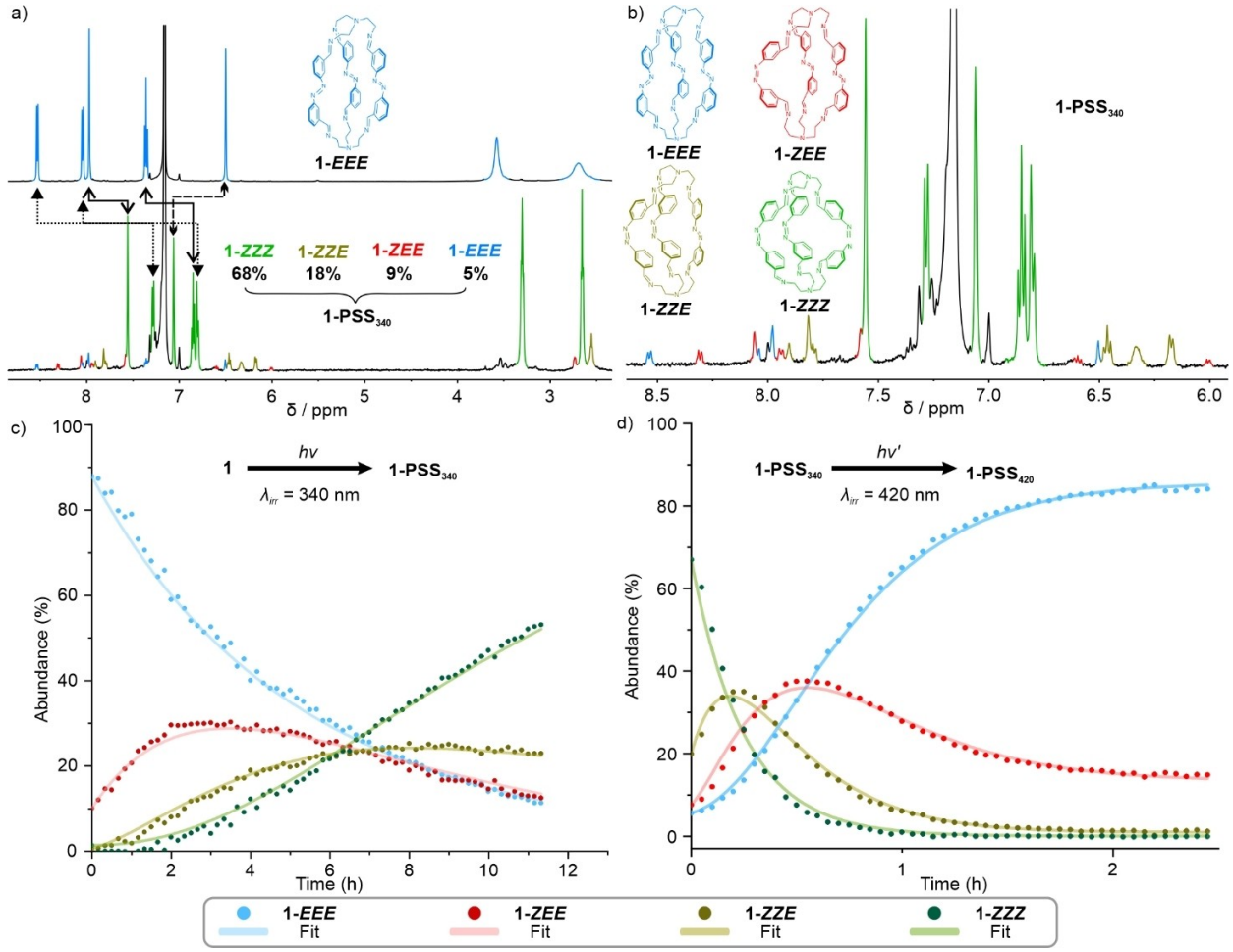

Figure 2. Isomerization studies of **1**. a) ^{1}H NMR spectra (1.1 mM, 500 MHz, 25 °C in C_6D_6) of pristine cage **1-*EEE*** (blue, top). No significant signal of any other cage isomer was observed. Upon ex situ irradiation (step I, λ_{irr} = 340 nm, 10 h) a mixture of different isomers **1-PSS$_{340}$** comprised of **1-*EEE*** (blue, 5 %), **1-*ZEE*** (red, 9 %), **1-*ZZE*** (brown, 18 %) and **1-*ZZZ*** (green, 68 %) is obtained. The arrows show the different chemical shifts observed for the isomers of **1-*EEE*** and **1-*ZZZ***. The overlapping arrows represent uncertainty on the corresponding signals for the of **1-*ZZZ*** isomer. b) Expansion of the aromatic region for the mixture **1-PSS$_{340}$**. c) Kinetic profile of sequence-specific isomerization of cage **1** under in situ irradiation with UV light (λ_{irr} = 340 nm). d) Kinetic profile of the sequence-specific *Z*/*E* isomerization of **1-PSS$_{340}$** under in situ irradiation with visible light (λ_{irr} = 420 nm).

oxybenzylamine (**2-OMeBnNH$_2$**, 1 equivalent) and the amine/imine exchange led to the partially open species **Open 1** (step II, Figures 3a–c and Supporting Figures S26–S34) was followed by ^{1}H NMR spectroscopy. By choosing **2-OMeBnNH$_2$** as the nucleophile, we were able to clearly follow the NMR signals of the formation of the new species (4.96–4.76 ppm, Supporting Figure S26) as well as the consumption of the nucleophile (3.85 ppm Supporting Figure S26). The amine/imine exchange reaction proceeds spontaneously and the formation of **Open 1-PSS$_{340}$** is first observed by the appearance of the benzylimine methylene group signals attached to a ***Z*** azobenzene at 4.82–4.75 ppm (Figure 3b, Supporting Figure S26). Note that after 1 h, signals for the benzylimine methylene group attached to a ***E*** azobenzene in **Open 1** are observed at 4.96 ppm (Figure 3b, Supporting Figure S29) due to spontaneous thermal *Z*/*E* isomerization of the azobenzene units. After a reaction time of 120 h, a total amount of **Open 1** (*E* and *Z* isomers) was obtained in 46 % yield. To suppress the thermal *Z*/*E* isomerization, we performed the amine/imine exchange experiment of **1-*EEE*** and **2-OMeBnNH$_2$** (0.8 mmol in C_6D_6, 1 equivalent) under constant irradiation (λ_{irr} = 340 nm). After 42.7 h under these conditions, **Open 1** (*E* and *Z* isomers) was obtained in 59 % yield. However, it should be noted that even after this time the reaction was still not fully equilibrated (Supporting Figures S30–S34).

The kinetic profile of the amine/imine exchange (Supporting Figure S35) indicates that isomers **1-*ZZZ*** and ***1-ZZE*** have similar reactivities, with rate constants of 3.06×10^{-3} min^{-1} and 3.48×10^{-3} min^{-1}, respectively. Due to the low abundance of **1-*ZEE*** and its fast thermal relaxation by double bond isomerization, it is not actively involved in the amine/imine exchange. The overall reaction rate of **Open 1-PSS$_{340}$** which is obtained by considering all isomers of **1** as a single species is 2.10×10^{-3} min^{-1}.

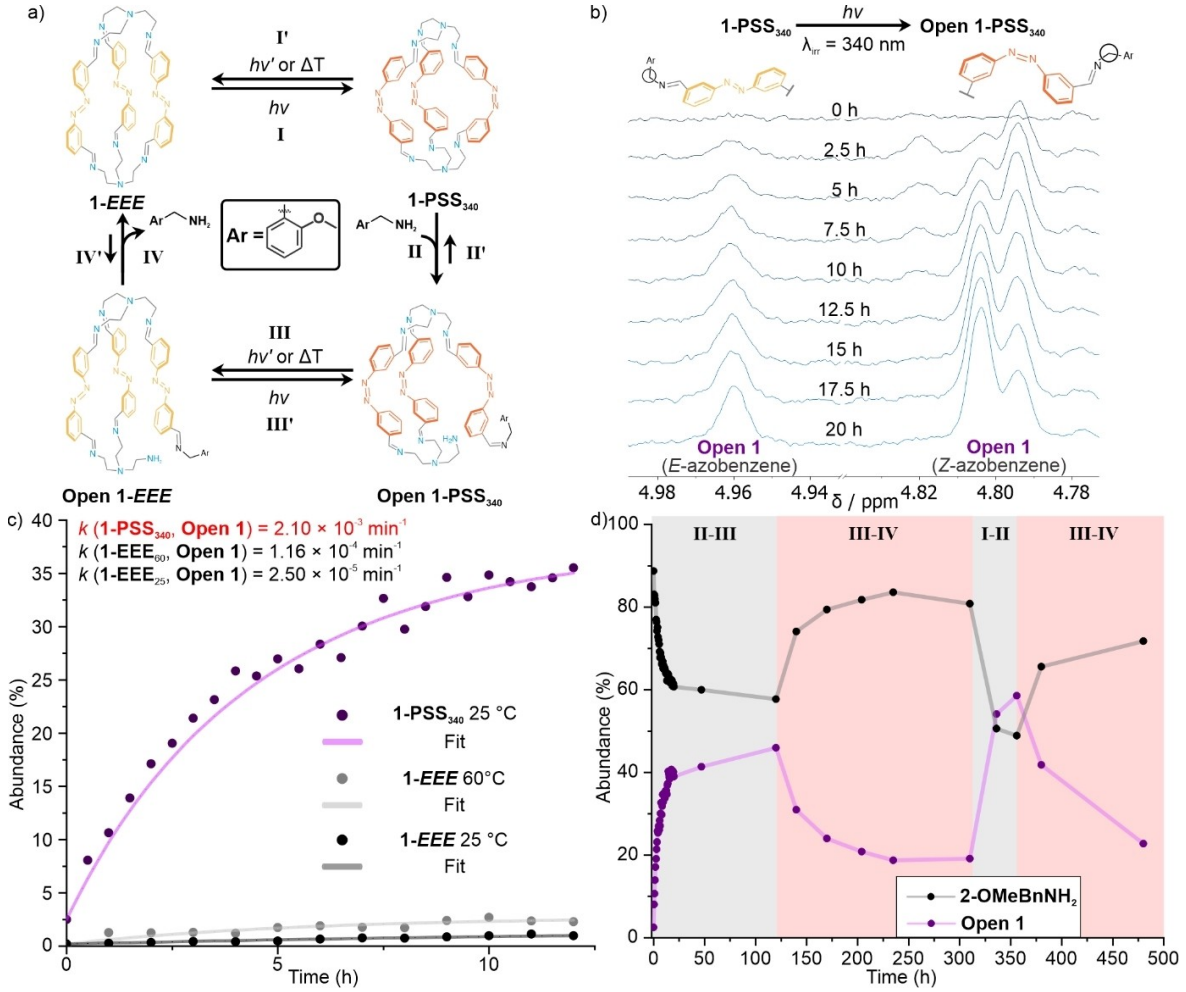

Figure 3. Light-induced cage-opening/closing cycle. a) Opening/closing cycle for **1** in steps I–IV. For each step, the reverse reaction is indicated as step I′–IV′. b) Evolution of a partial ^{1}H NMR spectrum (from top to bottom) during amine/imine exchange between **1-PSS$_{340}$** and **2-OMeBnNH$_2$** for 20 h (0.8 mM, 500 MHz, 25 °C in C_6D_6). c) Comparison of the intermolecular amine/imine exchange between **1** and **2-OMeBnNH$_2$** before switching (black and grey) and after switching (purple). d) Kinetic profiles of the opening/closing cycle of **1** with **2-OMeBnNH$_2$** (black) as a competing nucleophile. The intermolecular amine/imine exchange between an irradiated sample **1-PSS$_{340}$** and **2-OMeBnNH$_2$** was monitored for 120 h at room temperature in the dark (cage "opening", step II, grey background). Subsequent heating at 60 °C for 190 h (red background) promotes *Z*/*E* isomerization (step III) and intramolecular amine/imine exchange (step IV) as reflected in a decrease of **Open 1** and an increase of **2-OMeBnNH$_2$**. A second cycle is triggered with UV irradiation (λ_{irr} = 340 nm, 20 h, room temperature, grey area) which promotes *E*/*Z* isomerization (step I) and intermolecular amine/imine exchange (step II) simultaneously. After allowing the mixture to equilibrate for 24 h at room temperature in the dark, a second increment in the concentration of **Open 1** and a decrease in **2-OMeBnH$_2$** was observed as a result of the intermolecular amine/imine exchange in step II. Finally, the concentration of **Open 1** decreases again after heating at 60 °C for 120 h (red area, steps III and IV).

Step II′. Open 1-PSS$_{340}$→1-PSS$_{340}$ endergonic intramolecular amine/imine exchange

A kinetic analysis for the intramolecular amine/imine exchange from **Open 1-*ZZZ*** and **Open 1-*ZZE*** to **1-*ZZZ*** and **1-*ZZE*** (Supporting Figure S33) revealed that the rate constants are 6.21×10^{-4} min^{-1} and 1.45×10^{-4} min^{-1}, respectively. These results, together with the ones discussed in Step II, indicate that the reactivities of the switched *Z* isomers are comparable, suggesting that it is not necessary to fully switch the constrained trimer to obtain an enhancement of the reaction rate.

Step III. Open 1-PSS$_{340}$→Open 1-EEE population of the high-energy state

Similar to the relaxation process from **1-PSS$_{340}$→1-*EEE*** (step I′), the *Z*→*E* isomerization of the azobenzenes in **Open 1-PSS$_{340}$** and unreacted **1-PSS$_{340}$** occurs spontaneously and can be promoted by heat or visible light (λ_{irr} = 420 nm, Figure 3d, Supporting Figures S36–S40). The product of this chemical transformation is **Open 1-*EEE***, which is barely accessible in the endergonic amine/imine exchange of **1-*EEE*** and **2-OMeBnNH$_2$**. The pathway provided by switching cage **1** in steps I→III is an effective bypass to generate high-energy compound **Open 1-*EEE***. Thus, our system operates out-of-equilibrium by facilitating the formation of

the disfavored product in an intermolecular amine/imine exchange by light.

Step III′. Open 1-EEE→Open 1-PSS$_{340}$ isomerization of the high-energy state

Analogously to step I′, **Open 1-*EEE*** can be isomerize back to **1-PSS$_{340}$** using UV light irradiation (λ_{irr} = 340 nm, Supporting Figures S41–45).

Step IV. Open 1-EEE→1-EEE exergonic intramolecular amine/imine exchange

For the final step in the cage opening cycle, the system is found initially in an out-of-equilibrium distribution because of step III. Consequently, the spontaneous intramolecular amine/imine exchange takes place, regenerating **1-*EEE*** and releasing **2-OMeBnNH$_2$**. Heating of the mixture at 60 °C for 190 h leads to an observable decrease in the concentration of **Open 1-*EEE*** from an abundance of 48 % to 21 %. An increase of **2-OMeBnNH$_2$** is also observed. The yield for this step (**Open 1-*EEE*→1-*EEE***) is ≈60 % (Figure 3d, Supporting Figures S46–49). Since we now have **Open 1-*EEE*** in higher abundance, further irradiation of the closed system triggered another cage opening cycle. This was performed by irradiating with UV light for 13 h (λ_{irr} = 340 nm, Figure 3d, Supporting Figures S46–49) to promote a second cage opening. The yield for the conversion of **1** to **Open 1** in the second cycle is ≈45 %, which is observed by the increase of the overall abundance of **Open 1** from 21 % to 59 % in the mixture. Prolonged heating successfully completed the second cage opening cycle with a yield of ≈55 % for the reaction **Open 1-*EEE*→1-*EEE***, decreasing the overall abundance of **Open 1** to 23 %. It is noteworthy that after completing the two cycles, no signs of degradation of **1** were observed. Furthermore, the ability of cage **1** to incorporate compounds from the mixture and release it upon external stimuli can be considered as a method for the uptake and release[63] of nucleophiles.

Step IV′. 1-EEE→Open 1-EEE endergonic intermolecular amine/imine exchange

To further investigate the dependence of imine reactivity on strain in cage **1**, **2-OMeBnNH$_2$** (1 equivalent) was added to a sample containing **1-*EEE*** (0.8 mM in C_6D_6). Minor changes in the ^{1}H NMR spectra were observed after a reaction time 12 h of at 25 °C (Figure 3c, Supporting Figure S50) with <1 % yield and a reaction rate of 2.50×10^{-5} min^{-1}. Even at an elevated temperature of 60 °C (Figure 3c, Supporting Figure S51) only 2.5 % yield is observed with a reaction rate of 1.16×10^{-4} min^{-1}. The kinetic analysis shows that the irradiated sample (**1-PSS$_{340}$→Open 1**, Supporting Figure S27) has an observed reaction rate of 2.10×10^{-3} min^{-1}, which is 84 times higher than the non-irradiated sample (**1-*EEE*→Open 1-*EEE***, supporting Figure S50). When **1-*EEE*** is left to react with **2-OMeBnNH$_2$** for more than 100 h at 60 °C (Supporting Figure S52), it reaches an equilibrium forming 12 % of **Open 1**.

We were able to estimate the energy difference between the observed amine/imine exchanges using the obtained reaction rates (Supporting Table S1, Supporting Figure S53). For **1-*EEE*** and **Open 1-*EEE***, this energy difference is ≈9.1 kJ mol^{-1}. Since the maximum concentration of **Open 1** that was obtained from Step II and III is 60 %, and after step IV we observe a decrease to 20 %, were able to estimate that, in Step IV, the released energy associated to the cage closing is ≈3.6 kJ mol^{-1}.

This evidence indicates that the dynamic imine equilibrium is coupled to the isomerization of constrained cage **1**. To further confirm that the influence in the rate acceleration originates from the strain build-up in the cage and not from electronic or steric effects, the amine/imine exchange between the unconstrained switchable imine **4** was subjected to the same analysis.

The amine/imine exchange of both **4-*E*** and **4-*Z*** with **2-OMeBnNH$_2$** that generates **5-*E*** and **5-*Z***, respectively, (Figure 4, Supporting Figures S54 and S55) was investigated and only minor differences in the exchange rate of the linear imine compared to cage **1** were observed. The reaction rates for the amine/imine exchange between **2-OMeNH$_2$** and **4-*E* and 4-*Z*** are 3.62×10^{-3} mM^{-1} min^{-1} and 2.70×10^{-3} mM^{-1} min^{-1}, respectively. This indicates that isomerization of the azobenzene in an unconstrained system has no significant impact on the dynamic amine/imine equilibrium compared to the constrained system **1**.

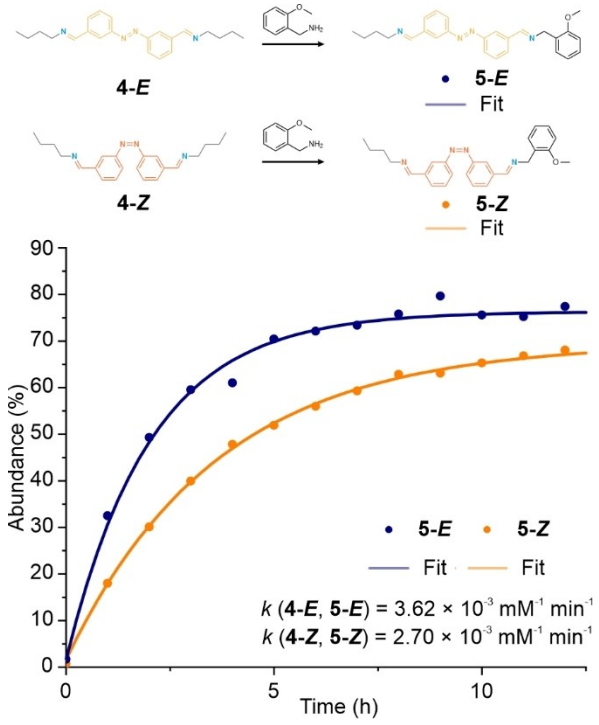

Figure 4. Influence of *E*/*Z* isomerization on the amine/imine exchange in an unconstrained system. Kinetic profiles of the reaction between the isomers of **4** (**4-*E***, blue and **4-*Z***, orange) with **2-OMeBnNH$_2$**.

Step V. Light-induced cage-to-cage transformation

Based on the light-induced opening/closing cycle of cage **1**, we evaluated if our system could undergo a cage-to-cage transformation. We found that in the case of the ditopic isophthalaldehyde **6**, the cage-to-cage transformation with **1-*EEE*** is a thermodynamically favorable but kinetically hindered process that leads to the formation of cage **2** (Figure 5, Supporting Figures S56, S57). This transformation was studied using a mixture of **1-*EEE*** (0.8 mM), **6** (1.2 mM, 1.5 equivalents) in C_6D_6 (saturated with water) that was heated in the dark at 60 °C for 230 h (Figure 5, Supporting Figure S56). Under these conditions, the formation of cage **2** was insignificant even though small signals for the hydrolyzed cage were observed in the ^{1}H NMR spectrum (step V′, Figure 5, Supporting Figure S56). However, when the same sample was irradiated with UV light (λ_{irr} = 340 nm, Figure 5, 22 h) at room temperature. A formation of 41 % of cage **2** was observed and after 290 h of keeping the irradiated sample in the dark at room temperature.

Additionally, the cage-to-cage transformation directly from the irradiated sample was studied using a mixture of **1-PSS$_{340}$** (0.8 mM in water-saturated C_6D_6) to which aldehyde **6** (1.2 mM, 1.5 equivalents) was added and the reaction was monitored in the dark at room temperature by ^{1}H NMR. Immediate formation of hydrolyzed open cage was observed (Supporting Figure S57), followed by the appearance of the characteristic signal of cage **2**, as well as the signals for the azobenzene **3**, both of which increased constantly at room temperature. Further heating of the sample increased the formation of cage **2**, even when all the azobenzenes in the mixture were converted into the *E* isomer. This can be due to the "closing" of the precursors of **2** that eventually are converted into cage **2**. Unlike the opening/closing cage cycle, the cage-to-cage transformation is not reversible, since cage **2** is thermodynamically more stable than cage **1**.

Conclusion

We showed experimentally that photoresponsive macrobicyclic imine cage **1** can be reversibly switched between the thermodynamically most stable state **1-*EEE*** and its high-energy *Z* isomers **1-*ZEE***, **1-*ZZE***, and **1-*ZZZ*** without losing its connectivity. The photo-induced alteration of self-assembled cage **1** changes not only the shape and dimensions of the molecule, but also its thermodynamic and kinetic stability. As a result, the exchange rates for the irradiated cage **1-PSS$_{340}$** with a competing nucleophile are roughly two orders of magnitude larger compared to the non-irradiated cage **1-*EEE***. By *Z*→*E* isomerization of **Open-1-PSS$_{340}$**, the concentration/population of **Open 1-*EEE*** is increased above the equilibrium level, thereby generating an out-of-equilibrium state. We utilized this principle to enable a kinetically hindered cage-to-cage transformation.

We envision that this operational principle for caged-based molecular machines will be a valuable tool for sophisticated manipulations of self-assembled molecular architectures based on dynamic chemistry. These dynamic and responsive materials can be used to promote energetically demanding transformation of constrained dynamic

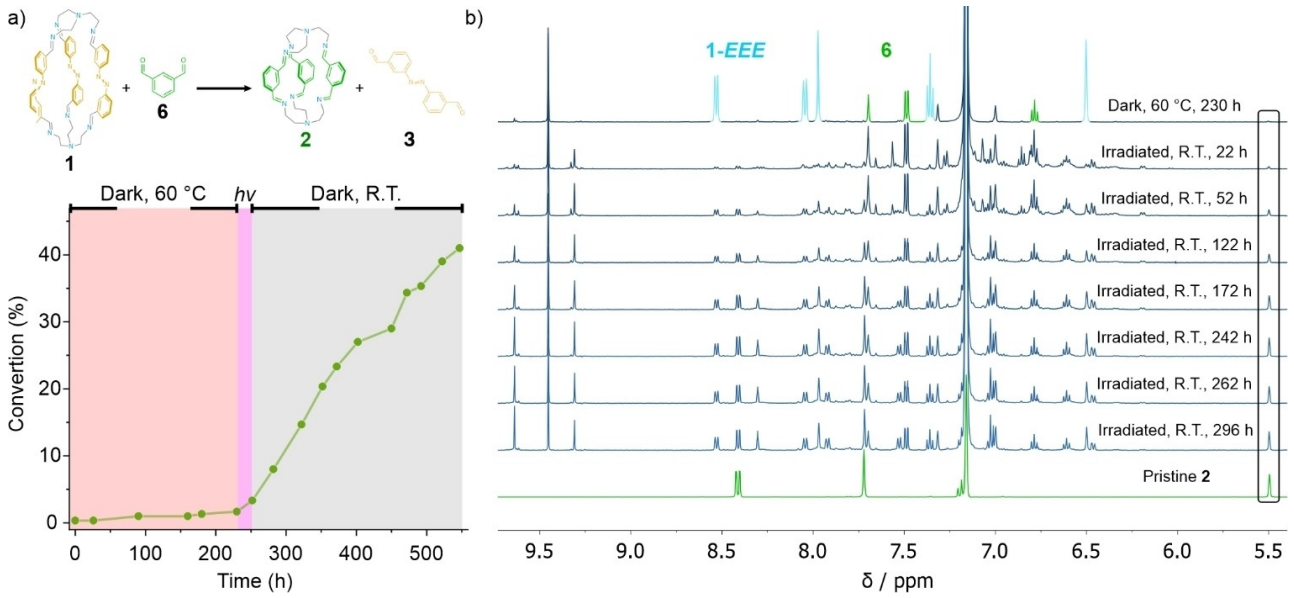

Figure 5. Light-induced cage-to-cage transformation. a) Kinetic traces of cage **2** under different conditions: 230 h of heating at 60 °C in the dark (red area), 22 h of irradiation with UV light (λ_{irr} = 340 nm, R.T., purple area) and, 290 h at room temperature, in the dark after irradiation (grey area). b) Evolution of a partial ^{1}H NMR spectrum (from top to bottom) of the light-induced cage-to-cage transformation. The first spectrum (top) represents the mixture of **1** and **6** after 230 h of heating at 60 °C. The next spectrum represents the same mixture after 22 h of irradiationwith UV light (λ_{irr} = 340 nm, room temperature) and the following spectrum represents the progression of this mixture after irradiation (in the dark at room temperature). The final spectrum is of pristine **2** for comparison.

compounds in a controlled and reversible manner. For example, the cage opening/closing cycle explored here might be a valuable tool to avoid product inhibition in cage catalysis, control uptake and release of nucleophiles with light, drug release and modulate transient dissipative self-assemblies with high spatiotemporal control.

Acknowledgements

The authors gratefully acknowledge financial support from the European Union (H2020 Excellent Science—Marie Skłodowska-Curie Actions) under grant number 838280 (S.C.), the Horizon 2020 Framework Program (ERC Advanced Investigator Grant No. 694345 to B.L.F.), the Ministry of Education, Culture and Science of the Netherlands (Gravitation Program No. 024.001.035 to B.L.F.) and Alexander von Humboldt-Stiftung (Alexander von Humboldt Foundation)—Feodor Lynen grant (M.K.). The authors thank R.J.L. Sneep for the HRMS measurements, P. van der Meulen and Dr. J. Kemmink for the support with NMR measurements, as well as Dr. A. Lubbe, Dr. R. Costil, Dr. A. Ryabchun and Dr. Q. Zhang for fruitful discussions.

Conflict of Interest

The authors declare no conflict of interest.

Data Availability Statement

The data that support the findings of this study are available from the corresponding author upon reasonable request.

Keywords: Dynamic Covalent Chemistry · Molecular Machines · Photoswitches · Self-Assembly · Out-Of-Equilibrium Chemistry

[1] D. S. Goodsell, *The Machinery of Life*, Springer New York, New York, **2009**.
[2] M. Schliwa, *Molecular Motors*, Wiley-VCH, Weinheim, **2002**.
[3] D. R. S. Pooler, A. S. Lubbe, S. Crespi, B. L. Feringa, *Chem. Sci.* **2021**, *12*, 14964–14986.
[4] J.-P Sauvage, *Molecular Machines and Motors*, Springer, Berlin, **2001**.
[5] A. Coskun, M. Banaszak, R. D. Astumian, J. F. Stoddart, B. A. Grzybowski, *Chem. Soc. Rev.* **2012**, *41*, 19–30.
[6] V. Balzani, A. Credi, F. M. Raymo, J. F. Stoddart, *Angew. Chem. Int. Ed.* **2000**, *39*, 3348–3391; *Angew. Chem.* **2000**, *112*, 3484–3530.
[7] W. R. Browne, B. L. Feringa, *Nat. Nanotechnol.* **2006**, *1*, 25–35.
[8] S. Krause, B. L. Feringa, *Nat. Chem. Rev.* **2020**, *4*, 550–562.
[9] V. Balzani, M. Venturi, A. Credi, *Molecular Devices and Machines—A Journey into the Nano World*, Wiley-VCH, Weinheim, **2003**.
[10] R. Herges, *Chem. Sci.* **2020**, *11*, 9048–9055.
[11] S. Amano, S. Borsley, D. A. Leigh, Z. Sun, *Nat. Nanotechnol.* **2021**, *16*, 1057–1067.
[12] E. Moulin, L. Faour, C. C. Carmona-Vargas, N. Giuseppone, *Adv. Mater.* **2020**, *32*, 1906036.
[13] M. Baroncini, S. Silvi, A. Credi, *Chem. Rev.* **2020**, *120*, 200–268.
[14] N. Koumura, R. W. J. Zijlstra, R. A. van Delden, N. Harada, B. L. Feringa, *Nature* **1999**, *401*, 152–155.
[15] R. Wilcken, M. Schildhauer, F. Rott, L. A. Huber, M. Guentner, S. Thumser, K. Hoffmann, S. Oesterling, R. de Vivie-Riedle, E. Riedle, H. Dube, *J. Am. Chem. Soc.* **2018**, *140*, 5311–5318.
[16] J. Chen, F. K. C. Leung, M. C. A. Stuart, T. Kajitani, T. Fukushima, E. van der Giessen, B. L. Feringa, *Nat. Chem.* **2018**, *10*, 132–138.
[17] R. Eelkema, M. M. Pollard, J. Vicario, N. Katsonis, B. S. Ramon, C. W. M. Bastiaansen, D. J. Broer, B. L. Feringa, *Nature* **2006**, *440*, 163–163.
[18] D. Dattler, G. Fuks, J. Heiser, E. Moulin, A. Perrot, X. Yao, N. Giuseppone, *Chem. Rev.* **2020**, *120*, 310–433.
[19] Y. Feng, M. Ovalle, J. S. W. Seale, C. K. Lee, D. J. Kim, R. D. Astumian, J. F. Stoddart, *J. Am. Chem. Soc.* **2021**, *143*, 5569–5591.
[20] Y. Qiu, Y. Feng, Q. H. Guo, R. D. Astumian, J. F. Stoddart, *Chem* **2020**, *6*, 1952–1977.
[21] C. Cheng, P. R. McGonigal, S. T. Schneebeli, H. Li, N. A. Vermeulen, C. Ke, J. F. Stoddart, *Nat. Nanotechnol.* **2015**, *10*, 547–553.
[22] M. Canton, J. Groppi, L. Casimiro, S. Corra, M. Baroncini, S. Silvi, A. Credi, *J. Am. Chem. Soc.* **2021**, *143*, 10890–10894.
[23] W. R. Feringa, B. Browne, *Molecular Switches*, Wiley-VCH, Weinheim, **2011**.
[24] R. D. Astumian, *Nat. Nanotechnol.* **2012**, *7*, 684–688.
[25] D. G. Blackmond, *Angew. Chem. Int. Ed.* **2009**, *48*, 2648–2654; *Angew. Chem.* **2009**, *121*, 2686–2693.
[26] M. Kathan, S. Hecht, *Chem. Soc. Rev.* **2017**, *46*, 5536–5550.
[27] Y. Munekage, M. Hashimoto, C. Miyake, K.-I. Tomizawa, T. Endo, M. Tasaka, T. Shikanai, *Nature* **2004**, *429*, 579–582.
[28] P. D. Boyer, *Biochim. Biophys. Acta Bioenerg.* **1993**, *1140*, 215–250.
[29] R. Göstl, A. Senf, S. Hecht, *Chem. Soc. Rev.* **2014**, *43*, 1982–1996.
[30] M. Herder, J.-M. Lehn, *J. Am. Chem. Soc.* **2018**, *140*, 7647–7657.
[31] D. N. Barsoum, V. C. Kirinda, B. Kang, J. A. Kalow, *J. Am. Chem. Soc.* **2022**, *144*, 10168–10173.
[32] M. Kathan, S. Crespi, N. O. Thiel, D. L. Stares, D. Morsa, J. de Boer, G. Pacella, T. van den Enk, P. Kobauri, G. Portale, C. A. Schalley, B. L. Feringa, *Nat. Nanotechnol.* **2022**, *17*, 159–165.
[33] H. Lee, J. Tessarolo, D. Langbehn, A. Baksi, R. Herges, G. H. Clever, *J. Am. Chem. Soc.* **2022**, *144*, 3099–3105.
[34] A. Singh, P. Verma, D. Samanta, A. Dey, J. Dey, T. K. Maji, *J. Mater. Chem. A* **2021**, *9*, 5780–5786.
[35] W. Liu, J. F. Stoddart, *Chem* **2021**, *7*, 919–947.
[36] T. Murase, S. Sato, M. Fujita, *Angew. Chem. Int. Ed.* **2007**, *46*, 5133–5136; *Angew. Chem.* **2007**, *119*, 5225–5228.
[37] S. J. Wezenberg, *Chem. Lett.* **2020**, *49*, 609–615.
[38] A. F. W. Kenedy, R. G. Dinardi, L. L. Fillbrook, W. A. Donald, J. E. Beves, *Chem. Eur. J.* **2022**, *28*, e202104461.
[39] A. B. Grommet, M. Feller, R. Klajn, *Nat. Nanotechnol.* **2020**, *15*, 256–271.
[40] D. Zhang, T. K. Ronson, Y.-Q. Zou, J. R. Nitschke, *Nat. Rev.* **2021**, *5*, 168–182.
[41] P. Li, Z. Sun, Y. Zuo, C. Yu, X. Liu, Z. Yang, L. Chen, E. Fu, W. Wang, J. Zhang, Z. Liu, J. Hu, S. Zhang, *J. Am. Chem. Soc.* **2022**, *144*, 1342–1352.
[42] B. Moosa, L. O. Alimi, A. Shkurenko, A. Fakim, P. M. Bhatt, G. Zhang, M. Eddaoudi, N. M. Khashab, *Angew. Chem. Int.*

Ed. **2020**, *59*, 21367–21371; *Angew. Chem.* **2020**, *132*, 21551–21555.
[43] H. Wang, S. Fang, G. Wu, Y. Lei, Q. Chen, H. Wang, Y. Wu, C. Lin, X. Hong, S. K. Kim, J. L. Sessler, H. Li, *J. Am. Chem. Soc.* **2020**, *142*, 20182–20190.
[44] K. Tian, S. M. Elbert, X.-Y. Hu, T. Kirschbaum, W.-S. Zhang, F. Rominger, R. R. Schröder, M. Mastalerz, *Adv. Mater.* **2022**, *34*, 2202290.
[45] M. Kathan, F. Eisenreich, C. Jurissek, A. Dallmann, J. Gurke, S. Hecht, *Nat. Chem.* **2018**, *10*, 1031–1036.
[46] Q.-Z. Yang, Z. Huang, T. J. Kucharski, D. Khavostichenko, J. Chen, R. Boulatov, *Nat. Nanotechnol.* **2009**, *4*, 302–306.
[47] T. J. Kucharski, Z. Huang, Q.-Z. Yang, Y. Tian, N. C. Rubin, C. D. Concepcion, R. Boulatov, *Angew. Chem. Int. Ed.* **2009**, *48*, 7040–7043; *Angew. Chem.* **2009**, *121*, 7174–7177.
[48] S. Akbulatov, Y. Tian, E. Kapustin, R. Boulatov, *Angew. Chem. Int. Ed.* **2013**, *52*, 6992–6995; *Angew. Chem.* **2013**, *125*, 7130–7133.
[49] M. E. Belowich, J. F. Stoddart, *Chem. Soc. Rev.* **2012**, *41*, 2003–2024.
[50] J.-M. Lehn, *Chem. Soc. Rev.* **2007**, *36*, 151–160.
[51] P. T. Corbett, J. Leclaire, L. Vial, K. R. West, J. L. Wietor, J. K. M. Sanders, S. Otto, *Chem. Rev.* **2006**, *106*, 3652–3711.
[52] K. Acharyya, P. S. Mukherjee, *Angew. Chem. Int. Ed.* **2019**, *58*, 8640–8653; *Angew. Chem.* **2019**, *131*, 8732–8745.
[53] H. Wang, Y. Jin, N. Sun, W. Zhang, J. Jiang, *Chem. Soc. Rev.* **2021**, *50*, 8874–8886.
[54] S. la Cognata, A. Miljkovic, R. Mobili, G. Bergamaschi, V. Amendola, *ChemPlusChem* **2020**, *85*, 1145–1155.
[55] Z. Yang, J. M. Lehn, *J. Am. Chem. Soc.* **2020**, *142*, 15137–15145.
[56] L. Ratjen, G. Vantomme, J.-M. Lehn, *Chem. Eur. J.* **2015**, *21*, 10070–10081.
[57] E. Nieland, J. Voss, A. Mix, B. Schmidt, *Angew. Chem. Int. Ed.* **2022**, *61*, e202212745; *Angew. Chem.* **2022**, *134*, e202212745.
[58] V. W. L. Gunawardana, T. J. Finnegan, C. E. Ward, C. E. Moore, J. D. Badjić, *Angew. Chem. Int. Ed.* **2022**, *61*, e202207428; *Angew. Chem.* **2022**, *134*, e202207418.
[59] D. del Giudice, M. Valentini, G. Melchiorre, E. Spatola, S. di Stefano, *Chem. Eur. J.* **2022**, *28*, e202200685.
[60] T. Hasell, X. Wu, J. T. A. Jones, J. Bacsa, A. Steiner, T. Mitra, A. Trewin, D. J. Adams, A. I. Cooper, *Nat. Chem.* **2010**, *2*, 750–755.
[61] F. T. Szczypiński, S. Bennett, K. Jelfs, *Chem. Sci.* **2021**, *12*, 830–840.
[62] K. Ono, N. Iwasawa, *Chem. Eur. J.* **2018**, *24*, 17859–17868.
[63] V. Lemieux, S. Gauthier, N. R. Branda, *Angew. Chem. Int. Ed.* **2006**, *45*, 6820–6824; *Angew. Chem.* **2006**, *118*, 6974–6978.

Manuscript received: October 2, 2022
Accepted manuscript online: December 1, 2022
Version of record online: January 19, 2023